Int. J. Heat Mass Transfer. Vol. 36, No. 1, pp. 177–182, 1993
Printed in Great Britain

0017-9310/93 $5.00 + 0.00

Natural convection in the cranked thermosyphon

G. S. H. LOCK and D. LADOON
Department of Mechanical Engineering, University of Alberta, Edmonton, Alberta, Canada T6G 2G8

(*Received* 7 *May* 1991 *and in final form* 17 *January* 1992)

Abstract—The paper presents the results of an experimental investigation of the heat transfer characteristics of the cranked, tubular thermosyphon under single phase conditions. Using water in a small scale rig, data have been obtained for $10^{5.9} < Ra < 10^{7.5}$, and have been plotted in the usual form of Nu vs Ra. The effect of Rayleigh number on Nusselt number suggests three flow regimes: for $Ra \leqslant 10^{6.5}$, a laminar, impeded regime is generally indicated; for $Ra > 10^{7.15}$, the data suggest a turbulent boundary layer regime; between these regimes is a third which has the characteristics of a short-lived fully-mixed turbulent regime.

INTRODUCTION

EVER SINCE the Perkins tube established the concept of the tubular thermosyphon a century ago [1], the device has seen an increasing number of applications. In essence, all of these take advantage of a single simple feature; namely, the ability of the device to transmit along its length convective fluxes which are much greater than the conductive flux under the same thermal boundary conditions. It is well known that the convective fluxes are attributable to circulation in the tube, and that this circulation is caused by thermal or Archimedean buoyancy forces.

Many of the early applications, and indeed many current applications, are based upon a straight tube heated at one end and cooled at the other. This simple arrangement limits use to situations in which the heat source and sink may be thus connected. There are other situations in which the size, shape and location of the source and sink demand the use of nonlinear tubes. In a cold region context, these include the freezing of soil around piles and poles [2]; beneath roads, airstrips and berms [3]; de-icing of marine structures [4]; de-icing of bridges [5]; and the storage of food [6].

Very little, if any, work has appeared on the cranked or offset thermosyphon illustrated schematically in Fig. 1. As indicated, it consists of two parallel sections, one heated and one cooled, separated by a third which is neither heated nor cooled. To the best of our knowledge, no study has been made of its heat transfer characteristics in either the single-phase or two-phase form. To help repair this deficiency, the present paper provides the results of an experimental study of the cranked thermosyphon in its most conservative form; namely, under single phase conditions. The purpose of the paper is to determine the basic thermal behaviour of a water-filled device in relation to a suggested flow model, and to explore the effect of thermosyphon geometry on this behaviour.

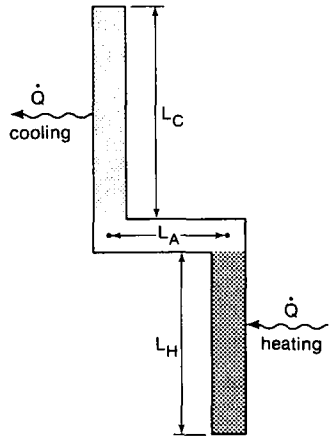

FIG. 1. Schematic of a cranked, tubular thermosyphon.

THE RIG

The rig is shown schematically in Fig. 2. It was constructed from two 80 cm lengths of 1.98 cm inner diameter copper tube having a wall thickness of 2 mm. The cooled (upper) section was surrounded by four equal and independent cooling jackets through which water from the building mains flowed. No attempt was made to measure the rate of heat extraction by the cooling jackets; under the steady conditions studied, it was equal to the net heat supply rate.

The heated (lower) section was also divided into four equal lengths, each being wrapped with electric heating tape. As indicated, these were wired in parallel and supplied with electricity from the building mains. This arrangement permitted adjustments in the local heat flux, and thus provided some control of axial variations in wall temperature. Before winding on the heating tape, the bare copper tube was wrapped in electrical insulating tape. After the heating tape was installed, the entire section was enclosed in a thick cylinder of fibreglass insulation.

NOMENCLATURE

D	tube diameter
k	thermal conductivity
L	tube length
Nu	Nusselt number
$\dot{Q}$	heat flux
Ra	Rayleigh number
T	temperature.

Greek symbols

β	thermal expansion coefficient
κ	thermal diffusivity
ν	momentum diffusivity.

Subscripts

A	adiabatic
C	cooled
H	heated.

Extending 6 cm beyond the open ends of the heated and cooled sections were short elbow pieces between which was fitted the adiabatic section. As indicated in Fig. 2, the adiabatic section and elbow pieces were also wrapped in a thick insulating cover. The offset, or length, of the adiabatic section, measured between the vertical tube centerlines, was altered by simply changing the distance between the elbow pieces. The lengths of the heated and cooled sections were changed by altering the length of styrofoam pistons or plugs inserted as shown in the figure. Each piston ensured that the thermosyphon was shut down over the length it occupied.

Temperature was measured throughout with copper constantan thermocouples, the signals from which were measured on a digital thermometer connected to the sensors via a switching box. Thermocouples were located on the outside of the heated and cooled section tubes every 2 cm on four equidistant rows around the circumference. Each tube wall temperature was taken as the average of twelve or more representative local values. The room air temperature was also recorded. Gross electrical power for each of the four lengths of heated section were measured in the usual way with an ammeter and voltmeter.

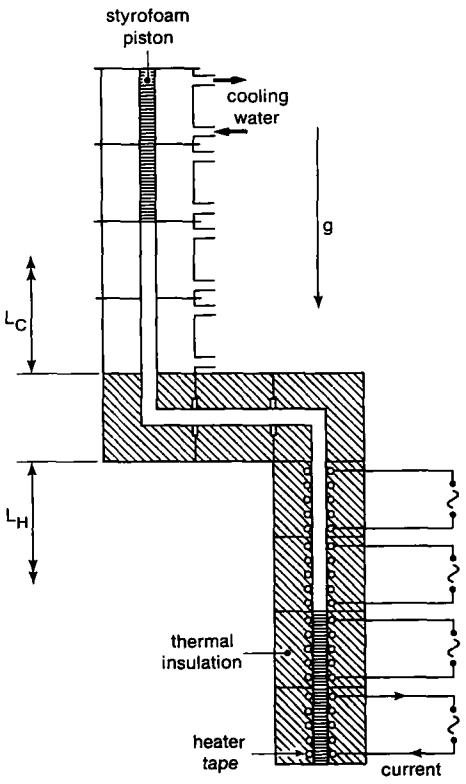

FIG. 2. Schematic of rig.

PROCEDURE

Prior to undertaking the main series of experiments, the heated section was calibrated in order that heat leakage from each length could be calculated under given conditions. This was accomplished with the heated section filled with a styrofoam piston, the power then supplied being lost entirely to the atmosphere. A plot of power thus supplied versus the temperature difference between the tube wall and the room air provided a quantitative estimate of the heat leakage. This quantity was subtracted from the gross supply rate during an experiment, the net value being taken as the heat transfer rate to, through, and from the thermosyphon. Since the leakage was found to be only a small fraction of the supply rate, and the tube wall temperature is furthest from the room temperature, no attempt was made to estimate the heat lost or gained in the insulated 'adiabatic' section.

The procedure for the experiments proper was as follows. With the adiabatic length chosen and installed along with the styrofoam pistons appropriate to selected lengths of the heated and cooled sections, the apparatus was filled with water. The cooling jacket water valves were then opened and the electrical power set at a low value. The system was allowed to stabilize for a period of about one hour after which the temperature and power levels were scanned. As a result of these observations, fine adjustments were made in the cooling water flow rates and power supply levels so that a better approximation to isothermal tube walls could be made. A further period of at least two hours was then allowed and the adjustment procedure repeated if necessary. After the elapse of a sufficient time, typically about four hours, the tem-

Table 1. Test schedule

Test	L_H (cm)	L_C (cm)	L_A (cm)
1	40	40	4
2	40	40	8
3	40	40	20
4	40	40	40
5	20	20	8
6	80	80	8

$D = 1.98$ cm, $10^{5.9} < Ra < 10^{7.5}$, $3.2 < Pr < 6.4$.

perature and power levels were recorded. The procedure was then repeated following an increase in the power supplied. Relatively large increases in power enabled the full range of the test to be spanned quickly following which successively lower readings were taken at intermediate points. In this way, not only could a sufficient number of points be generated to create a continuous curve but the possibility of hysteretic behaviour could be checked; hysteresis was not observed.

The data were plotted in the usual form of Nusselt number versus Rayleigh number where

$$Nu = \frac{\dot{Q}}{\pi k L_H \theta} \tag{1}$$

and

$$Ra = \frac{\beta g \theta D^3}{\nu \kappa} \tag{2}$$

in which $\dot{Q}$ is the net heat flux, $\theta = T_H - T_C$ is the overall temperature difference, L_H is the length of the heated section and D is the tube (inner) diameter. The range of conditions covered and the tube geometries studied in six runs are given in Table 1. A formal error analysis was also undertaken. Uncertainty bands thus calculated are superimposed on the data presented in graphical form later.

DISCUSSION OF RESULTS

Flow models

Before attempting to interpret the experimental data it is worthwhile discussing the fluid circulation pattern within the thermosyphon. No previous studies have uncovered this pattern and no visualization experiments were attempted here. On the other hand, flow within the linear tubular thermosyphon has been studied extensively for orientations which vary between the vertical and the horizontal [7–10]. From these it has been established that vertical and near-vertical tubes exhibit a bipartite flow pattern: near the closed ends, the primary circulation consists of an annular refluent flow in which a central core moves towards the end while a surrounding annulus moves away from it; in the mid length region, however, the flow is bifilamental, each filament being created by an annulus gradually transforming into a core moving in the same direction. This pattern is illustrated in Fig. 3.

While bent tubes have not been studied visually, the linear flow model has shown that it may be adapted to non-linear situations. In the elbow thermosyphon, for example, bifilamental flow in a heated, horizontal tube may be reconciled with annular refluent flow in a cooled, vertical tube to create a composite pattern [11], at least under laminar conditions. A similar adaptation for the cranked thermosyphon is suggested in Fig. 4(a). The vertical tubes, here taken equal in length, are assumed to contain a basically annular flow while the horizontal adiabatic length provides an anti-symmetric reconciliation in the form of a bifilamental coupling flow in which the hotter fluid lies above the cooler. Each horizontal filament is thus formed from the annulus of one section but is transposed into the core of the other. Thus, as the lower and cooler horizontal filament approaches the mouth of the vertical heated section it turns downward to allow rising fluid from the annulus below to flow round behind it.

Also noted under laminar conditions [11], was the effect of tilting back the elbow thermosyphon, its orientation changing from an L to a V. This enabled the hot tongue leaving the initially-horizontal, heated section to remain close to the inner surface of the tube wall and thus oppose, and eliminate, the descending annulus in that region of the cooled section. A bifilamental loop filling the entire thermosyphon was thus produced. Figure 4(b) suggests this form of circulation in a cranked thermosyphon. More will be said about these patterns later.

Flow regimes

Figures 5 and 6 show the effect of Rayleigh number on Nusselt number for various tube geometries. In Fig. 5, the length–diameter ratio was fixed at 20:1 while the offset ratio L_A/D was varied in the range $2 < L_A/D < 20$. Also shown in the figure is a line representing experimental data obtained in a straight vertical tube (i.e. $L_A = 0$) filled with water and having the same length–diameter ratio [12]; these data were obtained with $L_H/L_C = 2$, but the effect of heated–cooled length ratio is weak, particularly for $L_H/L_C \leqslant 2$ [12, 13]. For lower Rayleigh numbers, e.g. $Ra < 10^{6.5}$ the curves are steeper. This is consistent with the gradual development of a laminar impeded regime as the Rayleigh number is lowered further. Such a regime has been clearly identified in the linear thermosyphon [7, 14, 15], and is attributable to the gradual propagation of viscous effects beyond a thin boundary layer until they fill the entire cross section of the tube; the buoyant motion of near-wall fluid is then impeded by the core flowing in the opposite direction.

Given the experimental uncertainty indicated, it is evident that the offset ratio has little effect on performance for $L_A/D \leqslant 4$ when $10^{6.3} < Ra < 10^{7.3}$. Under these conditions, the Rayleigh number also has little effect, thus signalling a brief regime of fully-

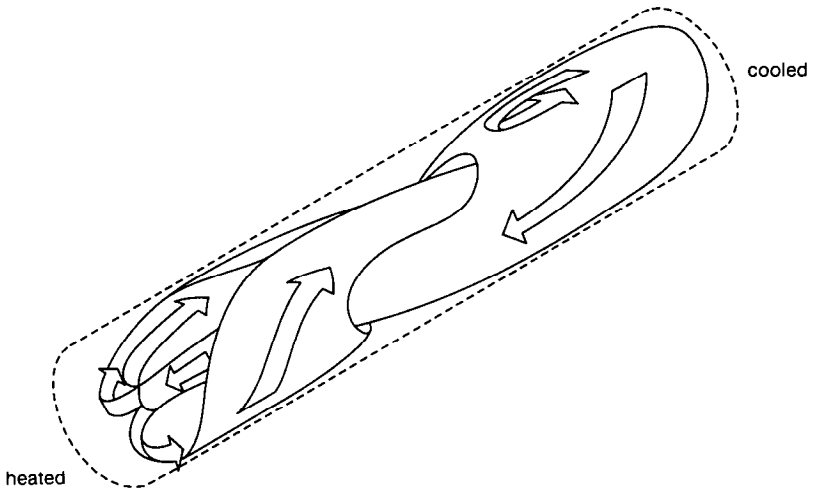

FIG. 3. Flow model of tilted linear thermosyphon.

mixed turbulence. Under comparable conditions, Martin [14] noted the transition from laminar-impeded flow to fully-mixed turbulence in a water-filled, linear open thermosyphon. Fully-mixed turbulence is characterized by slow, large-scale eddy motion in the absence of a well-defined mean circulation. Turbulent diffusion thus takes place over the entire cross section of the tube, suggesting a 'turbulent impeded' regime, except that longitudinal thermal energy exchange is mainly attributable to eddy motion; the heat transfer rate is essentially proportional to the temperature difference.

For $Ra < 10^{6.3}$, the steep slope suggests entry into a laminar impeded regime, while above $Ra = 10^{7.15}$ the slope of approximately 0.33 appears to indicate a turbulent boundary layer regime. This differs from the fully-mixed regime because the turbulence intensity is greater while the scale of turbulence is less; turbulent diffusion is largely restricted to near-wall boundary layers. Such a bifilamental structure is evidently created by the stronger stratification in the horizontal adiabatic length as the Rayleigh number increases. It was found that the data for $Ra > 10^{7.15}$ correlate roughly in the form

$$Nu = \frac{0.007Ra^{1/3}}{\left(1+\frac{L_A}{D}\right)^{0.226}}. \quad (3)$$

This assumes that the numerator represents behaviour when the offset is zero, but no data were obtained for $L_A/D \simeq 0$. It is not certain that the effect of L_A/D is monotonic in this range but it is evidently very small.

As the offset ratio is increased further, the short, constant Nusselt number section of the curve becomes even shorter and appears to vanish entirely for

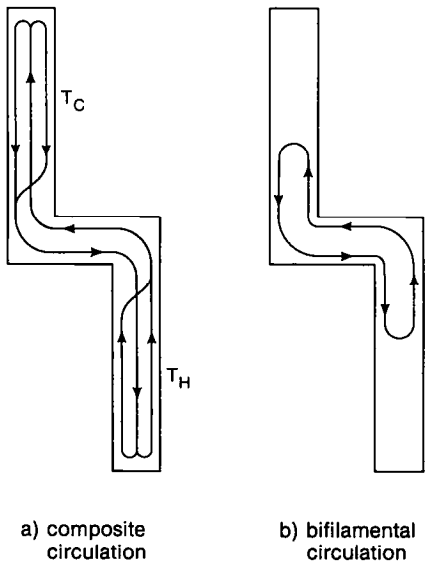

FIG. 4. Suggested flow models for cranked thermosyphon.

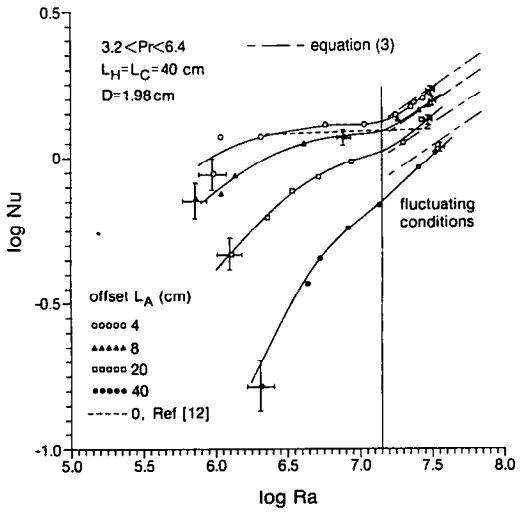

FIG. 5. Effect of offset on heat transfer.

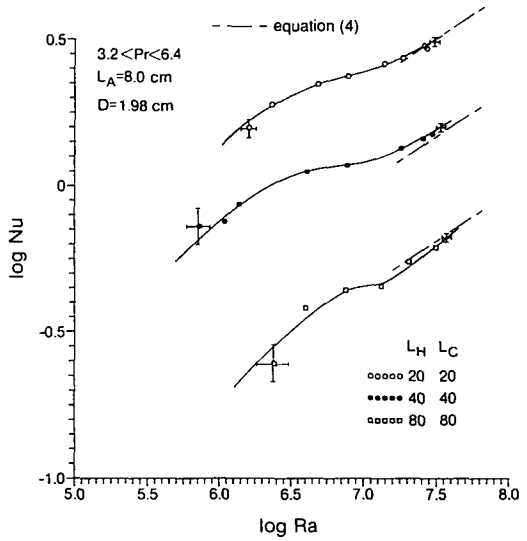

FIG. 6. Effect of length–diameter ratio on heat transfer.

$L_A/D \geqslant 20$. However, the laminar impeded regime and the turbulent boundary layer are both retained. Indeed $Ra \simeq 10^{7.15}$ appears to define the lower extent of the turbulent boundary layer regime and therefore $Ra \simeq 10^7$ may mark the point of transition to turbulence when the offset ratio is high. The flow models suggested in Fig. 4 both imply that the overall heat transfer rate between the two vertical sections would decrease with increasing offset ratio because lateral conduction between the two horizontal filaments grows with their length and thickness. Not surprisingly, the thicker filaments associated with laminar impeded flow produce a more rapid deterioration. This trend is seen in Fig. 5, and evidently continues until $L_A/D = 20$ when the upper limit of the impeded regime has been raised to $Ra = 10^{7.15}$.

It is important to note that all the data for $Ra > 10^{7.0}$ contained fluctuations exhibited as small oscillations in the heated wall temperature near the adiabatic section. No oscillations were evident for $Ra < 10^{7.0}$. At the same time, fluctuating conditions were invariably associated with a marked reduction in the power level of the heated length furthest from the adiabatic section. Typically, the power from this distant heater was only 5–10% of the other heater power. This type of behaviour is reminiscent of that observed in the linear thermosyphon at low Rayleigh numbers when a stagnant pool exists at the closed end [15]. The resolution of this paradox is suggested in Fig. 4(b) which depicts a purely bifilamental flow driven at high Rayleigh numbers by two mechanisms: the indirect buoyancy force created by the horizontal temperature gradient in the adiabatic section; and the direct buoyancy force acting in the reduced effective length of both vertical sections.

Such a pattern, in which flow in the adiabatic section is stably stratified, evidently accounts for the vigorous monotonic increase in Nusselt number seen in Fig. 5 when the Rayleigh number is increased beyond 10^7. The annular refluent pattern shown in Fig. 4(a) is difficult to justify in the presence of turbulence. Experience with the linear, vertical tube [7] indicates that a turbulent boundary layer flow does not occur unless the laminar-turbulent transition occurs in the laminar boundary layer regime, but the horizontal adiabatic section dramatically alters the situation in the cranked thermosyphon by creating stable stratification. Without this stratification, the destabilizing effect of the tongues of fluid entering the vertical sections leads to turbulence in both the core and the annulus, thus giving rise to fully-mixed flow. The turbulent boundary layers in the adiabatic section, however, exert a controlling influence on the overall flow pattern and, in particular, inhibit the onset of a fully-mixed flow.

Effect of tube geometry

In addition to the length of the adiabatic section discussed above, the full description of the tube geometry requires the specification of the heated and cooled section lengths. The effect of these lengths on system performance may, in general, be phrased in terms of two ratios: the heated–cooled length ratio L_H/L_C, and the heated length–diameter ratio L_H/D. In linear thermosyphons, the effect of the former is typically slight and its effect in a related study of the elbow thermosyphon was found to be completely absent [13]. For these reasons, it has not been studied here.

On the other hand, the effect of length–diameter ratio is typically strong. In general, it alters the heat transfer rate in two ways: through the change to an impeded regime when the tube becomes particularly long; and through the change in coupling mechanism in the mid-length region. Figure 6 uses the curve generated with $L_A/D = 4$ in Fig. 5 to explore the effect of the vertical tube length–diameter ratio. The lower slope section near $Ra = 10^7$ is evidently retained for an increased value of L_H/D but almost vanishes when L_H/D is decreased. This again suggests that $Ra \simeq 10^7$ marks the onset of instability with the result being a short-lived regime of fully-mixed turbulence for longer tubes but a direct transition to boundary layer turbulence for shorter tubes. In either event, the data for lower Rayleigh numbers again indicate laminar-impeded flow while those above indicate turbulent boundary layer flow. This leads to the suggestion that the principal effect of changing the length–diameter is to displace the overall curve in a monotonic fashion, but has little effect on the coupling mechanism. Apart from the fully-mixed flow in the vicinity of $Ra = 10^7$, the advective coupling mechanisms shown in Fig. 4 continue to apply; the composite pattern for laminar-impeded flow and the bifilamental pattern for turbulent boundary layer flow.

The strong monotonic effect of L_H/D seen in Fig. 6 is evidently the result of changes to the heated surface area in the Nusselt number. Given the flow pattern in Fig. 4(b), this area exerts little, if any, further influence

on the heat *flux* in the turbulent boundary layer regime once the flow fails to penetrate to the end of the tube. Only in the laminar impeded regime would L_H/D exert an effect on the heat flux. This explanation carries with it the implication that the Nusselt number should be inversely proportional to L_H when L_H is large. Correlation of the data in Fig. 6 for $Ra > 10^{7.15}$ reveals that

$$Nu = 0.164 Ra^{1/3}\left(\frac{D}{L_H}\right)^{1.19} \quad (4)$$

supporting the hypothesis of a turbulent boundary layer flow which does not penetrate into the deep region of the tube where circulation is much reduced.

CONCLUSIONS

The paper presents the results of an experimental investigation of the cranked, tubular thermosyphon. Using a configuration in which two diabatic, vertical tubes were separated by an adiabatic horizontal tube, data which reveal the heat transfer characteristics of the single phase device have been obtained. The data were plotted in the form of Nusselt number vs Rayleigh number with the latter being in the range $10^{5.9} < Ra < 10^{7.5}$. A systematic attempt was made to uncover the effect of the system geometry as represented by the offset ratio L_A/D and the heated length–diameter ratio L_H/D.

The heated length–diameter ratio was found to have the expected monotonic effect: the heat transfer rate decreased as the length–diameter ratio increased, the precise relationship suggesting turbulent boundary layer flow for $Ra \geqslant 10^{7.0}$.

The effect of the offset ratio was more complex. With $L_A/D \leqslant 4$, the parameter had little effect on heat transfer rate. The Nu–Ra curve then appeared to be divided into three different flow regimes. For $Ra \leqslant 10^{6.3}$, the steepness of the curve suggested the upper reaches of a laminar impeded regime in which the flow pattern consists of annular refluence in the vertical sections coupled through a bifilamental pattern in the horizontal section. Although not confirmed visually, this composite circulation pattern is consistent with similar adaptations in linear and nonlinear thermosyphons operating in the laminar impeded regime.

For $Ra \gtrsim 10^{7.0}$, the slope of the curves suggested a turbulent boundary layer flow in which the primary flow is a single (bifilamental) loop extending part way into each vertical section. Again unconfirmed visually, this pattern is consistent with observed reductions in the heat supplied to the deep regions of the vertical tubes; it also offers an explanation of the steepening slope of the Nu–Ra curve as Ra increased beyond $10^{7.0}$.

Between the laminar impeded regime and the turbulent boundary layer regime was a third. This is a brief regime, the extent of which varies with both L_H/D and L_A/D. The Nusselt number varied little in this regime suggesting chaotic behaviour and large scale turbulence originating in instability in the upper reaches of the laminar impeded regime; at higher Rayleigh numbers this evidently degenerates into small scale turbulence in the turbulent boundary layer regime, as dictated by the stably-stratified bifilamental flow in the adiabatic section.

Acknowledgements—This work was undertaken with a research grant from the Natural Sciences and Engineering Research Council of Canada to whom we are indebted. We also wish to thank Mr L. Zhao and the technical staff of the Department of Mechanical Engineering, Messrs A. Muir, B. Cielin and T. Nord in particular.

REFERENCES

1. C. R. King, Perkins' hermetic tube boilers, *The Engineer* **152,** 405–406 (1931).
2. E. D. Waters, Arctic tundra frozen by heat pipes, *Oil Gas J.* 122–125 (1975).
3. K. C. Cheng and J. P. Zarling, Applications of heat pipes and thermosyphons in cold regions, *Proc. 7th Int. Heat Pipe Conf.*, Minsk (1990).
4. Anon, First ship with practical de-icing system, *Zosen* **26**(7), 26 (1981).
5. C. H. Wilson, A demonstration project for de-icing of bridge decks, *Bridge Engng* **1,** 189–197 (1978).
6. M. Fukuda, F. Tsuchiya, K. Ryokai, M. Mochizuki and K. Mashiko, Development of an artificial permafrost storage using heat pipes, *Proc. 7th Int. Heat Pipe Conf.*, Minsk (1990).
7. F. J. Bayley and G. S. H. Lock, Heat transfer characteristics of the closed thermosyphon, *J. Heat Transfer* **87,** 30–40 (1965).
8. G. S. H. Lock, *The Tubular Thermosyphon.* Oxford University Press, Oxford (1992).
9. G. S. H. Lock and J.-C. Han, Buoyant laminar flow of air in a long, square-section cavity aligned with the ambient temperature gradient, *J. Fluid Mech.* **207,** 489–504 (1989).
10. G. S. H. Lock and J. D. Kirchner, Some characteristics of the inclined, closed tube thermosyphon under laminar conditions, *Int. J. Heat Mass Transfer* **35,** 165–173 (1992).
11. G. S. H. Lock and S. Park, A numerical study of the right-angled thermosyphon, *Proc. 10th Int. Conf. on Offshore Mechanics and Arctic Engng*, Stavanger (1991).
12. G. S. H. Lock and Y. Liu, The effect of geometry on the performance of the closed tube thermosyphon at low Rayleigh numbers, *Int. J. Heat Mass Transfer* **32,** 1175–1182 (1989).
13. G. S. H. Lock and D. Ladoon, Heat transfer in a right-angled thermosyphon, *Proc. 10th Int. Conf. on Offshore Mechanics and Arctic Engng*, Stavanger (1991).
14. B. W. Martin, Free convection in an open thermosyphon with special reference to turbulent flow, *Proc. R. Soc. London* **A230,** 502–530 (1955).
15. M. J. Lighthill, Theoretical considerations on free convection in tubes, *Q. J. Mech. Appl. Math.* **VI**(4), 398–439 (1953).